MicroRNA-7–regulated TLR9 signaling–enhanced growth and metastatic potential of human lung cancer cells by altering the phosphoinositide-3-kinase, regulatory subunit 3/Akt pathway

Lin Xu[a,*], Zhenke Wen[b,*], Ya Zhou[c], Zhongmin Liu[d], Qinchuan Li[d], Guangru Fei[e], Junmin Luo[a], and Tao Ren[d]

[a]Department of Immunology and [c]Department of Medical Physics, Zunyi Medical College, Guizhou 563000, China; [b]Institute for Immunobiology and Department of Immunology, Shanghai Medical College of Fudan University, Shanghai 200032, China; [d]Department of Respiratory Medicine and [e]Department of Cardiothoracic Surgery, East Hospital, Tongji University School of Medicine, Shanghai 200120, China

ABSTRACT **Recent evidence shows that microRNAs (miRNAs) contribute to the biological effects of Toll-like receptor (TLR) signaling on various cells. Our previous data showed that TLR9 signaling could enhance the growth and metastatic potential of human lung cancer cells. However, the potential role of miRNAs in the effects of TLR9 signaling on tumor biology remains unknown. In this paper, we first report that TLR9 signaling could reduce intrinsic miR-7 expression in human lung cancer cells. Furthermore, overexpression of miR-7 can significantly inhibit TLR9 signaling–enhanced growth and metastatic potential of lung cancer cells in vitro and in vivo. Notably, we identify phosphoinositide-3-kinase, regulatory subunit 3 (PIK3R3) as a novel target molecule of miR-7 in lung cancer cells by Western blotting and luciferase report assay. Further study shows that miR-7 inhibits the effects of TLR9 signaling on lung cancer cells through regulation of the PIK3R3/Akt pathway. These data suggest that miR-7 could act as a fine-tuner in regulating the biological effects of TLR9 signaling on human lung cancer cells, which might be helpful to the understanding of the potential role of miRNAs in TLR signaling effects on tumor biology.**

Monitoring Editor
J. Silvio Gutkind
National Institutes of Health

Received: Jul 16, 2012
Revised: Oct 9, 2012
Accepted: Oct 31, 2012

INTRODUCTION

Tumorigenesis of lung cancer is a complex, multistep process that includes cellular neoplastic transformation, resistance to apoptosis, autonomous growth signaling, emergence of a vascular supply, evasion of immunological surveillance, and the acquisition of invasive/metastatic properties. More and more functional molecules, which are expressed on lung cancer cells and involved in tumorigenesis, have been detected (Tsushima *et al.*, 2006; Wang *et al.*, 2006; Cammarota *et al.*, 2010). Recently a rapid accumulating body of literatures demonstrated that Toll-like receptors (TLRs), which are mainly expressed on immune cells and recognize a variety of pathogen-associated molecular patterns (Creagh and O'Neill, 2006; Xu *et al.*, 2010b), are also widely expressed on various tumor cells, including lung cancer cells (Droemann *et al.*, 2005; Huang *et al.*, 2005; Song *et al.*, 2006; Ioannou and Voulgarelis, 2011; Bhattacharya and Yusuf, 2012). Further studies showed that TLR agonist could alter the biological character of lung cancer cells; among its effects were promoting the proliferation and enhancing the metastatic potential of tumor cells in vitro and in vivo (He *et al.*, 2007; González-Reyes *et al.*, 2011; Min *et al.*, 2011). These results indicated that activation of TLR signaling in lung cancer cells could contribute to the growth and metastasis of tumor cells and is ultimately involved in tumor progression (Chen *et al.*,

This article was published online ahead of print in MBoC in Press (http://www.molbiolcell.org/cgi/doi/10.1091/mbc.E12-07-0519) on November 7, 2012.

*These authors contributed equally to this work.

Address correspondence to: Tao Ren (rentaosh@126.com).

Abbreviations used: BrdU, 5-bromo-2-deoxyuridine; CLL, chronic lymphocytic leukemia; DMSO, dimethyl sulfoxide; ELISA, enzyme-linked immunosorbent assay; FACS, fluorescence-activated cell sorting; FBS, fetal bovine serum; FITC, fluorescein isothiocyanate; H&E, hematoxylin and eosin; miR-7, microRNA-7; miRNA, microRNA; MTT, 3-(4,5-dimethylthiazol-2-yl)-2,5-diphenyltetrazolium bromide; ODNs, oligonucleotides; pAkt, phospho-Akt; PBS, phosphate-buffered saline; PBS-T, PBS plus 0.03% Tween 20; PI, propidium iodide; PIK3R3, phosphoinositide-3-kinase, regulatory subunit 3; RNAi, RNA interference; RT-PCR, real-time PCR; TLRs, Toll-like receptors; UTR, untranslated region.

2008b). However, the underlying mechanism remains to be fully elucidated.

MicroRNAs (miRNAs) have emerged as a major class of gene expression regulators, posttranscriptionally regulating gene expression through base pairing to partially complementary sites to prevent protein accumulation by repressing translation or by inducing mRNA degradation; they are linked to most biological functions, including tumor biology. miRNAs are differentially expressed in various human cancers and are believed to play important roles in tumor progression (Esquela-Kerscher and Slack, 2006). Furthermore, miRNA expression profiles have been found to be putative markers for improving cancer classification, diagnosis, and clinical prognostic information (Majumder and Jacob, 2011; Mínguez and Lachenmeyer, 2011). Recently increasing evidence showed that miRNAs also play critical roles in regulating the biological effects of TLR signaling pathway on various cells (Chen *et al.*, 2008a; Tserel *et al.*, 2009; Wendlandt *et al.*, 2012). As such, miR-147 and miR-21 could regulate biological effects of the TLR4 signaling pathway on immune cells (Liu *et al.*, 2009; Sheedy *et al.*, 2010). However, the possible role of miRNAs involved in the effect of TLRs on progression of cancer remains largely unknown.

Recent evidence demonstrated that human lung cancer cells express functional TLR9 molecules (Droemann *et al.*, 2005; Pinto *et al.*, 2011; Sorrentino *et al.*, 2011). TLR9 was also highly expressed in tumor mass from non–small cell lung cancer patients (Samara *et al.*, 2012). Consistently, our previous work showed that TLR9 agonist CpG oligonucleotides (ODNs) could promote the growth and metastatic potential of human lung cancer cells (Ren *et al.*, 2007, 2009; Xu *et al.*, 2009, 2010a). Most recently, other research work showed that the miR-17-92 cluster might regulate the biological effect of CpG ODNs on chronic lymphocytic leukemia (CLL) cells (Bomben *et al.*, 2012). However, whether miRNAs are involved in the effects of TLR9 signaling on lung cancer cells remains to be elucidated. Some new research showed that microRNA-7 (miR-7), a unique member of miRNAs, plays an important role in the progression of various tumors, including lung cancer (Kong *et al.*, 2011a,b; Saydam *et al.*, 2011). Mechanistic evidence showed that miR-7 could regulate the transduction of the Akt pathway, which is critical for growth and metastasis of tumor cells (Webster *et al.*, 2009; Fang *et al.*, 2012). Our previous data showed that the Akt pathway was critical for the effects of TLR9 signaling on lung cancer cells (Xu *et al.*, 2009). We therefore suspect that miR-7 might play a potential role in TLR9 signaling on the growth and metastatic potential of lung cancer cells.

In the present study, we observed the direct effect of TLR9 agonist CpG ODNs on the expression of intrinsic miR-7 in human lung cancer cells. Furthermore, we investigated the possible effect of miR-7 overexpression on the growth and metastasis of lung cancer cells and explored its possible mechanisms. Our findings indicated that miR-7 could act as fine-tuner in regulating TLR9 signaling–associated biological effects in human lung cancer cells, which might be helpful to the understanding of the potential role of miRNAs in tumor biology.

RESULTS

TLR9 signaling reduces the expression of miR-7 in human lung cancer cells

To elucidate the potential role of miR-7 in TLR9 signaling–stimulated lung cancer cells, we determined the expression of intrinsic miR-7 in TLR9 agonist CpG ODN–treated human lung cancer cells. As shown in Figure 1, A and B, we found that CpG ODNs could significantly reduce the expression level of miR-7 in 95D cells in a dose- and time-dependent manner ($p < 0.05$). To further confirm these results, we investigated the activity of miR-7 promoter in 95D cells stimulated with CpG ODNs. As shown in Figure 1C, we found that TLR9 signaling could significantly reduce the activity of miR-7 promoter in lung cancer cells ($p < 0.05$). To verify the effect of TLR9 signaling on the expression of miR-7, we also transiently transfected TLR9 RNA interference (RNAi) into 95D cells and observed the expression of miR-7 on these cells in response to CpG ODNs. We found that CpG-ODN treatment did not alter the expression level of intrinsic miR-7 in the TLR9 RNAi-transfected group (Figure 1D, $p > 0.05$), indicating TLR9 signaling was responsible for the reduced expression of intrinsic miR-7 in 95D cells in response to CpG ODNs. To confirm these data, we also applied the homodimerization inhibitory peptide MyD88 inhibitor (Ahmad *et al.*, 2007). We found that MyD88 inhibitor could also significantly abrogate the effect of CpG ODNs on miR-7 expression in 95D cells (Figure 1E, $p < 0.05$).

Our previous study showed that CpG ODNs could also enhance the proliferation and metastasis of TLR9-modifying 95C cells, which intrinsically expressed low levels of TLR9 (Ren *et al.*, 2007; Ren *et al.*, 2009). To further confirm the above phenomenon, we observed the expression level of miR-7 in TLR9-modifying 95C cells and in other human lung cancer cell lines (BE1, NCI-H727 and SPCA/I). Consistently, we found that CpG ODNs also obviously reduced the relative expression level of miR-7 in TLR9-modifying 95C cells and BE1, NCI-H727, and SPCA/I cells (Figure 1, F and G, $p < 0.05$). Combining these data suggested that TLR9 signaling could significantly reduce the expression of intrinsic miR-7 in lung cancer cells.

Overexpression of miR-7 impairs TLR9 signaling–enhanced growth of human lung cancer cells

Our previous data showed that TLR9 signaling could enhance the growth of human lung cancer cells (Ren *et al.*, 2009; Xu *et al.*, 2010a). To investigate whether miR-7 was involved in the effects of TLR9 signaling on human lung cancer cells, we investigated the direct effect of miR-7 on the growth of 95D cells enhanced by CpG ODNs. As shown in Figure 2, A and B, miR-7 could significantly impair the growth of 95D cells in vitro ($p < 0.5$), which was consistent with a previous report (Xiong *et al.*, 2011). Importantly, we found that miR-7 could also significantly impair the growth of 95D cells stimulated by CpG ODNs in vitro (Figure 2, A and B, $p < 0.05$). To confirm these results, we also performed the 5-bromo-2-deoxyuridine (BrdU) incorporation assay and found similar results (Figure 2, C and D, $p < 0.5$). In addition, we further analyzed the potential effect of miR-7 on the apoptosis and cell cycle entry of CpG ODN–stimulated 95D cells. We found that miR-7 had no significant effect on the early apoptosis of CpG ODN–stimulated 95D cells (Figure 2E, $p > 0.05$), whereas it significantly reduced the percentage of CpG ODN–stimulated 95D cells at S and G2/M stage, indicating that miR-7 could inhibit the cell cycle entry of CpG ODN–stimulated 95D cells (Figure 2F, $p < 0.05$).

To confirm the above phenomenon in vivo, we evaluated the effect of miR-7 on the growth of 95D cells enhanced by CpG ODNs in nude mice. Compared with scramble control, miR-7 could significantly inhibit the growth of 95D cells in vivo (Figure 3A, $p < 0.05$). Importantly, we found that miR-7 could also significantly inhibit the growth of 95D cells enhanced by CpG ODNs in vivo (Figure 3A, $p < 0.05$). Consistently, the survival time of CpG ODN–treated 95D-bearing nude mice was also significantly prolonged (Figure 3B, $p < 0.05$). Combining these data demonstrated that overexpression of miR-7 could inhibit the effect of TLR9 signaling on the growth of human lung cancer cells.

Overexpression of miR-7 reduces TLR9 signaling–enhanced metastatic potential of human lung cancer cells

Our previous data also showed that TLR9 signaling could enhance the metastatic potential of human lung cancer cells in vitro and

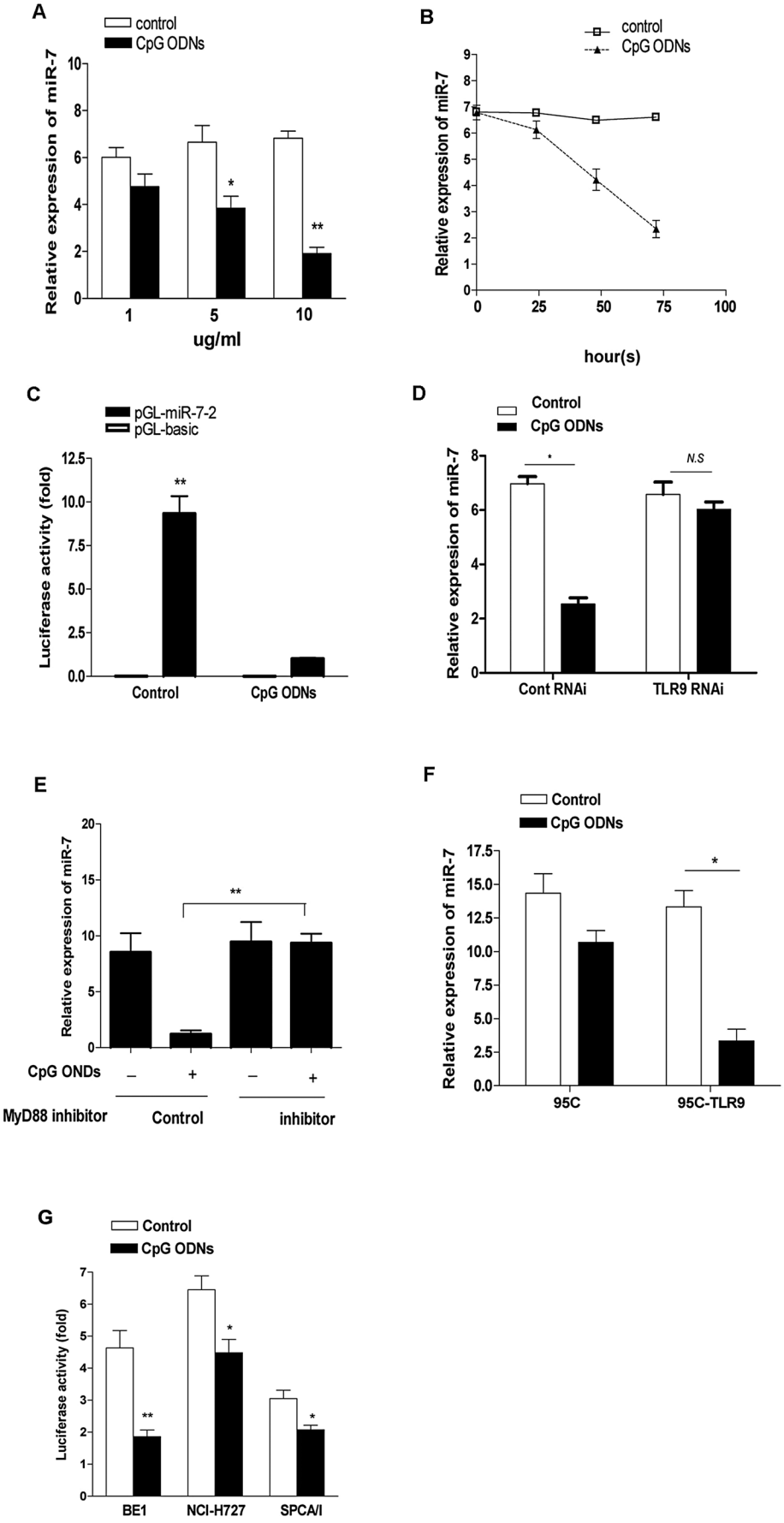

in vivo (Ren *et al.*, 2007; Xu *et al.*, 2009). Then, to further access the potential role of miR-7 in TLR9 signaling–enhanced progression of human lung cancer, we also detected the direct effect of miR-7 on the metastatic potential of 95D cells stimulated by CpG ODNs. As shown in Figure 4, A and B, a wound-healing assay showed that miR-7 could significantly reduce the migration of 95D cells in vitro ($p < 0.5$). Expectedly, miR-7 could also significantly reduce the migration of 95D cells enhanced by CpG ODNs in vitro (Figure 4, A and B, $p < 0.5$). To further confirm this finding, we also conducted a Transwell migration assay and found similar results (Figure 4C, $p < 0.05$). Furthermore, we found that miR-7 could significantly inhibit the invasive capacity of CpG ODN–stimulated 95D cells in vitro (Figure 4D, $p < 0.5$). Moreover, the secretion of IL-8, which is an important metastasis-associated molecule (Ren *et al.*, 2007) from CpG ODN–stimulated 95D cells also was obviously reduced in the miR-7–transfected group (Figure 4E, $p < 0.05$).

To confirm this finding, we further evaluated the possible effect of miR-7 on

FIGURE 1: TLR9 signaling reduced the expression of miR-7 in human lung cancer cells. (A) The 95D cells were treated with the indicated dose of CpG ODN or control CpG ODN. After 72 h, the expression level of miR-7 was detected by RT-PCR assay. (B) The 95D cells were treated with 10 μg/ml CpG ODN or control CpG ODN. The expression level of miR-7 was analyzed by RT-PCR assay at the indicated time points. (C) Plasmid pcMV-lacZ was transiently transfected into 95D cells with plasmid pGLmiR-7 Luc or pGLBasic. Then cells were cultured at 3×10^3 cells/well in a 24-well plate in the presence of 10 μg/ml CpG ODN. After 24 h, the activity of miR-7 promoter was determined by luciferase reporter assay. (D) The 95D cells were transiently transfected with TLR9 RNAi (100 nmol) or control RNAi (100 nmol) and then treated with10 μg/ml CpG ODN. After 72 h, the expression level of miR-7 was detected by RT-PCR assay. (E) The 95D cells were treated with 10 μg/ml CpG-ODN in the presence of 100 μm/ml control peptide (Control) or MyD88 inhibitor peptide (inhibitor) for 72 h. The expression level of miR-7 was analyzed by RT-PCR assay. (F and G) Human lung cancer cell line 95C, TLR9-modifying 95C, BE1, NCI-H727, and SPCA/I cells were treated with 10 μg/ml CpG ODN for 72 h. The expression level of miR-7 was then analyzed in each group of cells. One representative datum for three independent experiments is shown. *, $p < 0.05$; **, $p < 0.01$; N.S., no significance.

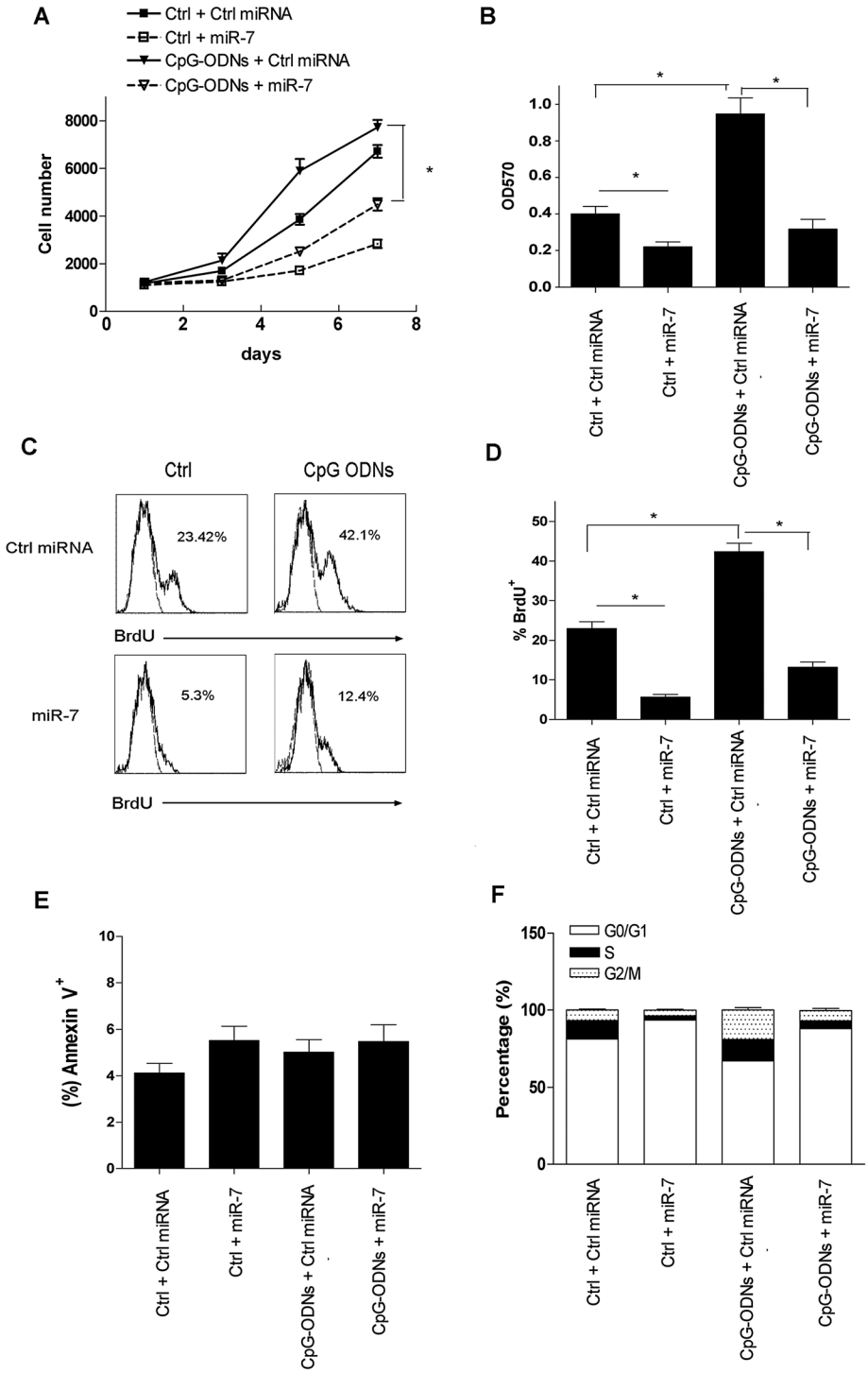

FIGURE 2: Overexpression of miR-7 impaired TLR9 signaling–enhanced growth of human lung cancer cells in vitro. A sample of 5×10^2 95D cells transiently transfected with miR-7 mimics or scramble control (10 nM) were cultured in the presence of 10 μg/ml CpG ODN. The cell count of each group was calculated at the indicated time point (A). After 72 h, the proliferation of cells was determined with MTT assay (B) or BrdU incorporation assay (C) and calculated (D). The early apoptosis (E) and cell cycle entry (F) of cells was also analyzed by FACS and calculated. Each bar represents the means (± SD) from eight nude mice in each group. *, $p < 0.05$.

the metastasis of 95D cells enhanced by CpG ODNs, using in vivo metastasis assay. As shown in Figure 4F, compared with the control groups, miR-7 could also effectively reduce the lung metastasis of 95D cells enhanced by CpG ODNs in vivo ($p < 0.05$). To confirm this data, we further observed the effect of miR-7 on the metastasis of 95D cells enhanced by CpG ODNs in a human lung cancer nude mice model. Consistently, similar results were obtained (Figure 4G, $p < 0.05$). Combining these data suggested that overexpression of miR-7 could reduce the effect of TLR9 signaling on the metastatic potential of human lung cancer cells.

miR-7 regulates the expression of phosphoinositide-3-kinase, regulatory subunit 3 (PIK3R3) in human lung cancer cells

To study the potential molecular mechanism through which miR-7 regulates the effects of TLR9 signaling on human lung cancer cells, we searched for miR-7 targets using computer-aided miRNA target prediction programs, including TargetScan 4, miRanda, and PicTar, and found 11 putative miR-7 target genes, including *EGFR*, *PIK3R3*, *IRS2*, *NXT2*, *RB1*, *RSBN1*, *PSME3*, *POLE4*, *SPATA2*, *HPCAL4*, and *SMARCD1*. To investigate the potential target of miR-7, which associated to TLR9 signaling, we detected the expression level of the putative targets in CpG ODN–treated 95D cells, using real-time PCR and Western blotting. As shown in Figure 5, A and B, we found that the expression level of PIK3R3 was particularly elevated in CpG ODN–treated 95D cells ($p < 0.05$). In contrast, there were no significant changes on the expression level of other genes ($p > 0.05$). Therefore we explored whether PIK3R3 was a potential target of miR-7 in 95D cells, using Western blotting. As shown in Figure 5C, we found that miR-7 could significantly reduce the expression of PIK3R3 protein in 95D cells. Moreover, we investigated the direct effect of miR-7 on the expression of PIK3R3, using a luciferase reporter assay. As shown in Figure 5D, miR-7 could suppress more than 80% activity for pLuc-PIK3R3–untranslated region (pLuc-PIK3R3-UTR) compared with vector control ($p < 0.05$).

To further confirm this finding, we also detected the effect of miR-7 on the expression of PIK3R3 in other human lung cancer cells, including BE1, NCI-H727, and SPCA/I cells. Consistently, the expression of PIK3R3 in BE1, NCI-H727, and SPCA/I cells was significantly reduced in the miR-7–transfected group (Figure 5E, $p < 0.05$). Combining these data suggested that miR-7 could effectively repress the expression of TLR9 signaling–associated molecule PIK3R3 in human lung cancer cells.

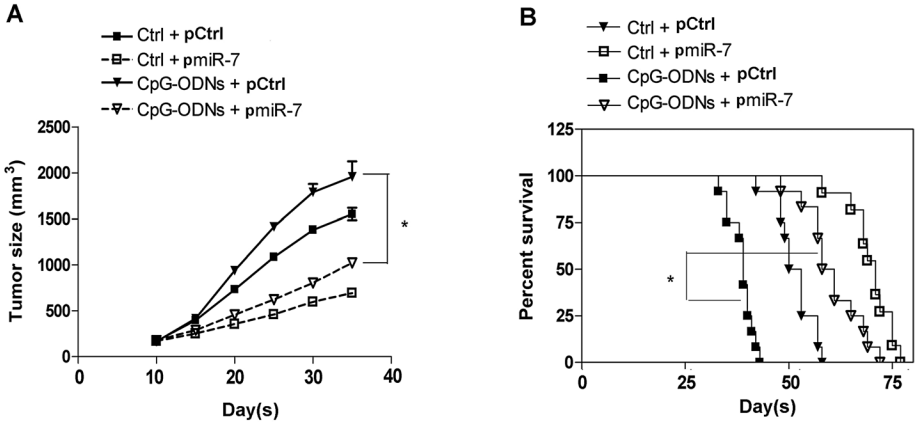

FIGURE 3: Overexpression of miR-7 impaired TLR9 signaling–enhanced growth of human lung cancer cells in vivo. (A) Groups of eight nude mice were challenged with 2×10^6 95D cells transiently transfected with 100 μg miR-7 expression vector (pmir-7) or control vector (pCtrl). After 5 d, the tumor-bearing mice were injected in situ with 100 μg of CpG ODN at 7-d intervals. The control group received an equal dose of the control CpG ODN. The tumor size of each group was observed. (B) The survival of each group was also obtained. Each symbol represents the means (± SD) from eight nude mice in each group. *, $p < 0.05$.

PIK3R3/Akt pathway is involved in the effect of TLR9 signaling on human lung cancer cells

Previous studies suggested that the PIK3R3/Akt pathway could contribute to the progression of cancers (Soroceanu *et al.*, 2007; Zhang *et al.*, 2007; Hu *et al.*, 2008). Our data reported above showed that TLR9 signaling could enhance the expression of PIK3R3 in human lung cancer cells. We therefore investigated whether the PIK3R3/Akt pathway was involved in the effect of TLR9 signaling on human lung cancer cells. As shown in Figure 6A, we found that CpG-ODN stimulation could effectively increase the expression of pAkt in 95D cells, which was consistent with our previous work (Xu *et al.*, 2009). Then we down-regulated the expression of PIK3R3 using a small interfering RNA and found that TLR9 signaling–enhanced expression of pAkt was significantly reduced in the PIK3R3 RNAi-transfected group in vitro (Figure 6B, $p < 0.05$). Importantly, we found that TLR9 signaling–enhanced growth of 95D cells was also significantly reduced in the PIK3R3 RNAi-transfected group in vitro (Figure 6, C and D, $p < 0.05$). To confirm this finding, we further down-regulated the transduction of the PIK3R3/Akt pathway, using Akt inhibitor. As expected, we found that Akt inhibitor could also significantly impair the effect of CpG ODNs on the growth of 95D cells (Figure 6, C and D, $p < 0.05$), indicating the PIK3R3/Akt pathway was involved in the effect of TLR9 signaling on 95D cells. To further verify these results, we also observed the effect of PIK3R3 down-regulation on the growth of 95D cells enhanced by TLR9 signaling in vivo. As shown in Figure 6E, the growth of CpG ODN–stimulated 95D cells was decreased in the PIK3R3 RNAi-transfected group compared with the control group ($p < 0.05$).

Next we investigated whether down-regulation of PIK3R3 could influence the metastatic potential of 95D cells enhanced by TLR9 signaling. As shown in Figure 7A, TLR9 signaling–enhanced invasion capacity of 95D cells in vitro was also significantly reduced in the PIK3R3 RNAi-transfected group ($p < 0.05$). A similar result was obtained in the Akt inhibitor treatment group (Figure 7A, $p < 0.05$). Finally, TLR9 signaling–enhanced metastasis of 95D cells in vivo was also significantly reduced in the PIK3R3 RNAi-transfected group (Figure 7B, $p < 0.05$). Combining these data suggested that the PIK3R3/Akt pathway was involved in TLR9 signaling–enhanced growth and metastatic potential of human lung cancer cells.

miR-7 regulated TLR9 signaling–enhanced growth and metastatic potential of human lung cancer cells via regulation of the PIK3R3/Akt pathway

Finally, we investigated whether miR-7 regulated TLR9 signaling–enhanced growth and metastatic potential of human lung cancer cells through regulation of the PIK3R3/Akt pathway. As shown in Figure 8A, we found that overexpression of miR-7 could effectively repress the expression of PIK3R3 in CpG ODN–stimulated 95D cells ($p < 0.05$). Consistently, the level of pAkt and phosphor-mTOR were also significantly reduced (Figure 8, B and C, $p < 0.05$), indicating that miR-7 could significantly reduce the transduction of the PIK3R3/Akt pathway in 95D cells stimulated by CpG ODNs.

To further confirm that miR-7 regulated the effect of TLR9 signaling on the growth and metastatic potential of human lung cancer cells mainly through repressing the expression of PIK3R3, we constructed the plasmid pcDNA3.1-PIK3R3 (termed pPIK3R3). We then cotransfected miR-7 into 95D cells with or without pPIK3R3 or control plasmids and found that the expression level of PIK3R3 on pPIK3R3-cotransfected groups increased significantly (Figure 9A, $p < 0.05$). Importantly, we found that the growth of 95D cells in vitro increased significantly in the pPIK3R3-cotransfected group compared with the miR-7–transfected group (Figure 9B, $p < 0.05$), indicating that overexpression of PIK3R3 could significantly reverse the inhibitory effect of miR-7 on TLR9 signaling–enhanced growth of 95D cells. Furthermore, the inhibitory effects of miR-7 on TLR9 signaling–enhanced invasion capacity of 95D cells in vitro were also significantly abrogated in the pPIK3R3-cotransfected group (Figure 9C, $p < 0.05$). These data suggested that miR-7 repressed the expression of PIK3R3 and successively altered the transduction of the PIK3R3/Akt pathway, which ultimately regulated TLR9 signaling–enhanced growth and metastatic potential of human lung cancer cells.

DISCUSSION

Recently accumulating data showed that miRNAs play critical roles in regulating TLR signaling pathways and their biological effects on immune cells and tumor cells (Rebane *et al.*, 2011; Kirigin *et al.*, 2012; Patron *et al.*, 2012). In our previous study, we found that TLR9 signaling could enhance the growth and metastatic potential of human lung cancer cells in vitro and in vivo (Ren *et al.*, 2007, 2009; Xu *et al.*, 2009, 2010a). In this study, we extended our previous finding by demonstrating that TLR9 signaling could significantly reduce the expression of intrinsic miR-7 in human lung cancer cells. Similar to others' results (Xiong *et al.*, 2011), we also found that miR-7 could regulate the growth and metastatic potential of human lung cancer cells. Most importantly, we found that overexpression of miR-7 caused an obvious reduction in TLR9 signaling–enhanced growth and metastatic potential of human lung cancer cells in vitro and in vivo. Combining our data suggested that down-regulation of intrinsic miR-7 could contribute to the biological effects of TLR9 signaling on human lung cancer cells. In recent research, it has been reported that TLR4 signaling could enhance the expression of miR-146a, which could subsequently regulate TLR4 signaling through repressing the expression of IL-1R–associated kinase 1(Nahid *et al.*, 2011).

Moreover, Ceppi and colleagues reported that TLR signaling–associated miR-155 could act as a part of a negative feedback loop that down-modulated inflammatory cytokine production in immune cells in response to TLR agonist (Ceppi *et al.*, 2009). To the potential role of miRNAs in TLR9 signaling, one research group has added the fact hat the miR-17-92 cluster could regulate TLR9 signaling on CLL cells (Bomben *et al.*, 2012). Thus these findings indicate that expression of specific miRNA molecules might play an intrinsic fine-tuning role in the regulation of TLR9 signaling in various cancer cells. In addition, we also found that TLR9 signaling could induce the repression of activity of miR-7 promoter in human lung cancer cells. However, the underlying mechanism through which TLR9 signaling reduces the expression of miR-7 still remains to be elucidated.

It is well known that the PI3K/Akt pathway is critical in tumor biology. Our previous study also showed that the Akt pathway was critical for TLR9 signaling–enhanced metastatic potential of human lung cancer cells (Xu *et al.*, 2009), and up-regulation of CDK2 conferred TLR9 signaling–enhanced growth of human lung cancer cells (Xu *et al.*, 2010a). Consistently, other work has shown that the Akt pathway was involved in the TLR9 signaling–mediated antiapoptotic effect (Lim *et al.*, 2012). Moreover, Akt signaling also can enhance the expression of CDK2 in tumor cells (Guo *et al.*, 2009; Lin *et al.*, 2012). Therefore it seems that the Akt pathway might be important for the effects of TLR9 signaling on lung cancer cells through different effectors. In the present study, using RT-PCR and Western blot assay, we also found that TLR9 signaling could enhance the expression of PIK3R3 in human lung cancer cells. Furthermore, we demonstrated by RNAi assay that the PIK3R3/Akt pathway was critical for TLR9 signaling–enhanced growth and metastatic potential of human lung cancer cells. Consistently, other evidence also showed that the PIK3R3/Akt pathway was important for biology of cancer cells (Zhang *et al.*, 2007; Soroceanu *et al.*, 2007), and that the PI3K/Akt pathway is involved in TLR9 signaling on other cells, such as macrophages and microglia cells (Ravindran *et al.*, 2010). Finally, there were some potential signaling adaptors linking TLRs to the serine/threonine kinases PI3K/Akt (Troutman *et al.*, 2012). Therefore the exact interaction between PIK3R3 and other PI3K family members or potential signaling molecules in the effects of TLR9 signaling on human lung cancer cells remains to be explored in successive studies.

Accumulating data show that miR-7 can regulate the biology of various tumor cells through repressing the expression of different target molecules (Webster *et al.*, 2009; Kong *et al.*, 2011a,b). In the current study, we first identified PIK3R3 as a novel target molecule of miR-7 in human lung cancer cells, using Western blot and luciferase assay. Furthermore, we reported that miR-7 could repress the expression of PIK3R3 and subsequently reduced the transduction of the Akt pathway, which ultimately regulated TLR9 signaling–enhanced growth and metastatic potential of human lung cancer cells. Similarly, Chen and colleagues reported that miR-199a could regulate TLR4 signaling in ovarian cancer cells through inhibiting the expression of IKKβ (Chen *et al.*, 2008a). Interestingly, one recent research work suggested that miR-7 could regulate the transduction of Akt pathway by regulating the expression of PIK3R2 in hepatocellular carcinoma (Fang *et al.*, 2012). Xiong and colleagues also showed that miR-7 could inhibit the growth of human non–small cell lung cancer A549 cells through targeting BCL-2 (Xiong *et al.*, 2011). These findings might support the fact that specific miRNA molecules could be an important intrinsic regulator through regulation of specific molecules in distinct tumor cells in different settings, which ultimately contributes to tumor biology. Undoubtedly, the observation on the possible role of miR-7 on primary human lung cancer, which was not investigated in the current study, was of value for validation of the critical role of miR-7 in the biological effects of TLR9 signaling on lung cancer cells in successive research work.

In all, our present study showed that the down-regulation of miR-7 contributed to TLR9 signaling–enhanced progression of human lung cancer through altering PIK3R3/Akt pathway transduction, suggesting that TLR9 signaling might contribute to the progression of tumor cells by altering the expression of specific miRNAs. These findings might be helpful to understanding the potential role of miRNAs in TLR signaling on tumor biology.

MATERIALS AND METHODS

Animals

Female BALB/c nude mice 5–6 wk of age were purchased from the Center of Experimental Animals, Fudan University (Shanghai, China). All animals were housed in the pathogen-free mouse colony at our institution, all animal experiments were performed according to the *Guidelines for the Care and Use of Laboratory Animals* (Ministry of Health, People's Republic of China, 1998), and all the experimental procedures were approved by the ethical guidelines of Shanghai Medical Laboratory Animal Care and Use Committee (permit number: 2010016).

Reagents and cell lines

The following ODNs were used and purchased from Integrated DNA Technologies (Coralville, IA): CpG ODN 2216 5′-GGGGGACGATCGTCGGGGG-3′; control, ODN 1612: 5′-GCTAGAGCTTAGGCT-3′. CpG ODN has a phosphorothioate backbone that provides a high degree of nuclease resistance. Human lung cancer cell line 95D cells, 95C cells, TLR9-modifying 95C cells, NCI-H727 cells, BE1 cells, and SPA/I cells were cultured at 37°C under 5% CO_2 in completed RPMI-1640 (Gibco, Grand Island, NY) medium containing 10% heat-inactivated fetal bovine serum (FBS) and supplemented with 2 mM glutamine, 100 IU/ml penicillin, and 100 µg/ml streptomycin sulfate. miR-7 mimics and scramble control were purchased from Applied Biosystems (Bedford, MA). PIK3R3 RNAi, TLR9 RNAi, and corresponding control RNAi were purchased from Novus Biologicals (Littleton, CO). Akt inhibitor IV was purchased from Merck. All other reagents were purchased from Sigma-Aldrich (St. Louis, MO), unless stated otherwise.

Real-time PCR assay

All reagents, primers, and probes were obtained from Applied Biosystems. A β-actin endogenous control was used for normalization. Reverse transcriptase reactions and real-time PCR (RT-PCR) were performed according to the manufacturer's protocols (Applied Biosystems, Foster, CA). RNA concentrations were determined with a NanoDrop instrument (NanoDrop Technologies, Wilmington, DE). One nanogram of RNA per sample was used for the assays. All RT reactions, including no-template controls and RT minus controls, were run in triplicate in a GeneAmp PCR 9700 Thermocycler (Applied Biosystems). Gene expression levels were quantified using the ABI Prism 7900HT sequence detection system (Applied Biosystems). Relative expression was calculated using the comparative threshold cycle method. The primers used for target genes are listed in Table 1.

Plasmid construction and preparation

The gene for the PIK3R3 (BC021622.1) were expanded by RT-PCR from human mRNA derived from 95D cells using a forward primer (5′-CGGAATTCCCTGTTCGGGTAGTTT) and a reverse primer (5′-GGGGTACCCCTTCCAGCTTAGTATGTC) and then subcloned into *Eco*RI and *Kpn*I sites of pcDNA3.1 vector (Invitrogen, San Diego, CA)

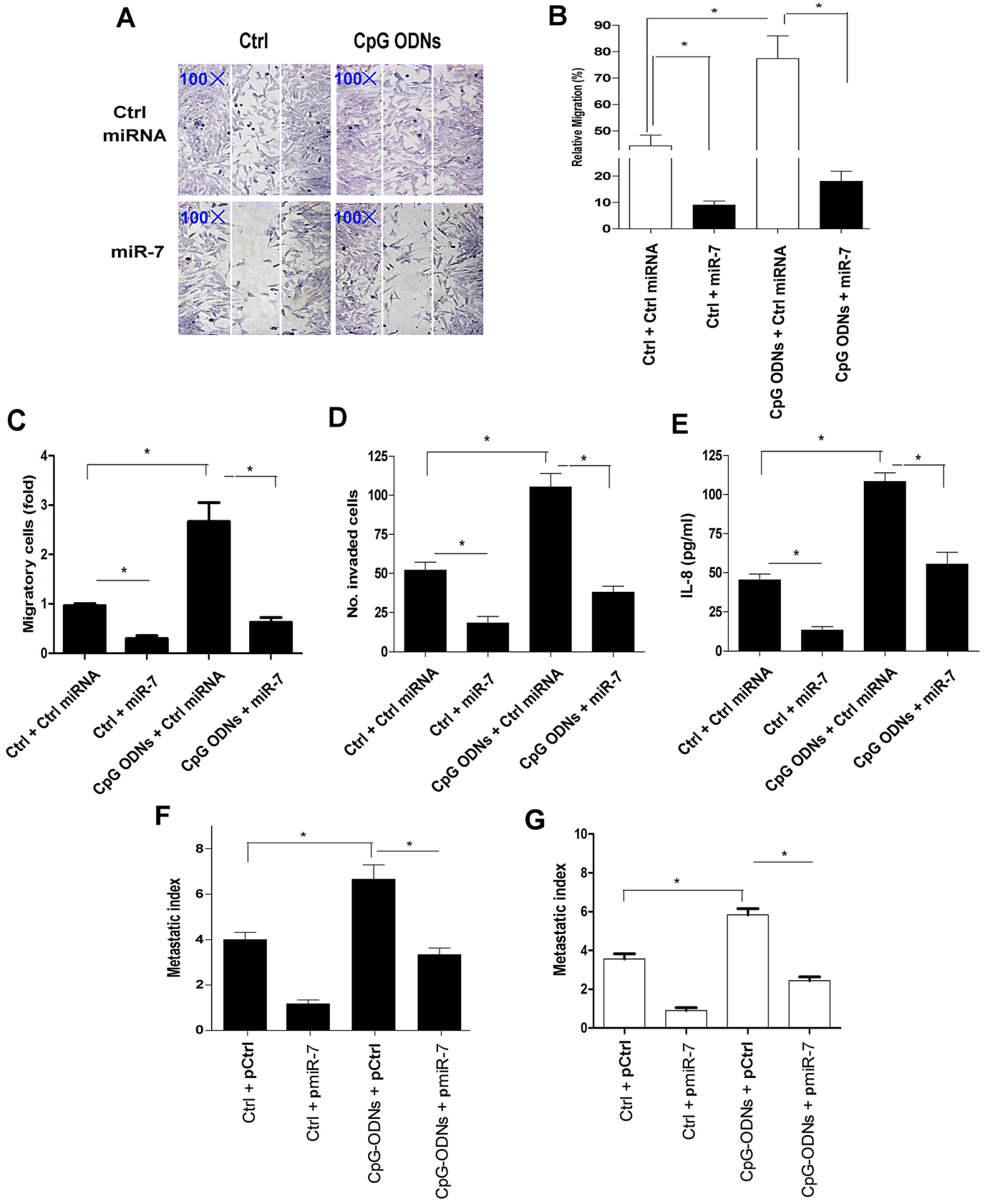

FIGURE 4: Overexpression of miR-7 reduced TLR9 signaling–enhanced metastatic potential of human lung cancer cells. The 95D cells transiently transfected with miR-7 mimics or scramble control (10 nM) were cultured in the presence of 10 μg/ml CpG ODN. (A) The migration of 95D cells was performed by scratch assay and observed with a microscope. The white line indicates the border of scratch wound at 0 h postwounding (magnification: 100×). One representative

to generate a pcDNA3.1-PIK3R3 plasmid (termed as pPIK3R3). For the construction of the plasmid pGLmiR-7 Luc, the promoter region (–1260 base pairs to 12 base pairs upstream) of miR-7 was amplified from DNA derived from 95D cells using a forward primer (5′-GGGGTACCCCGGTATTGCCAGTCTTC) and a reverse primer (5′-CGGCTAGCGTATCCAGGCCAGTT) and subcloned into *Kpn*I and *Nhe*I sites of pGL basic vector. The plasmid pMir-7 was constructed as previously reported (Reddy *et al.*, 2008). Pre–miR-7-2 with a 600–base pair flanking sequence was amplified from genomic DNA with sense (5′-GGAAGAGAGAAATGAGCCACTTGC) and antisense (5′-GTATTCCTGCCACAGTGGGGGATG) primers and then cloned into the pcDNA3.1 plasmid. Clone identity was verified using restriction digest analysis and plasmid DNA sequencing Endotoxin-free plasmids were obtained using Endofree plasmid mega kit (Qiagen GmbH, Hilden, Germany). These plasmids were then transiently transfected into the 95D cells using Lipofectamine 2000 (Invitrogen) in the following experiments according to the manufacturer's instruction.

Growth curve experiments

Growth curves were performed in duplicate in 24-well plates. A cell suspension was prepared by collecting cells by centrifugation. The cells were washed twice with RPMI-1640 medium, and a viable cell count was determined by trypan blue exclusion in a hemocytometer. Then 5×10^2 viable cells were seeded into a 96-well plate containing 1 ml of complete RPMI-1640 medium. Cell counts were performed at the indicated time points by removing the entire contents of one well with a Pasteur pipette, washing the well once with phosphate-buffered saline (Invitrogen, Mexico, CA), centrifuging the cells, discarding the supernatant, resuspending the cells in a known volume of RPMI-1640 medium, and counting the suspension in a hemocytometer. The data represent the average of duplicates of total cell numbers per well determined by multiplying the cell concentration times the volume resuspended.

Cell proliferation assays

The 95D cells transiently transfected with 10 nM miR-7 mimics or scramble control using Lipofectamine 2000 (Invitrogen) were seeded at 3×10^3 cells each well and incubated in the presence of CpG ODNs in the dose of 10 µg/ml at 37°C in 5% CO_2 in 96-well plates for 72 h. Assessment of cell proliferation was measured in terms of optical absorbance (OD) per well by a semiautomated tetrazolium-based colorimetric assay using 3-(4,5-dimethylthiazol-2-yl)-2,5-diphenyltetrazolium bromide (MTT). On day 3 of the stimulation, 20 µl of MTT solution (5 mg/ml) was added to each well and further incubated at 37°C for an additional 4 h. Supernatants were then removed from the wells, and 120 µl of 20% dimethyl sulfoxide (DMSO) was added. Each well was mixed thoroughly for 10 min to dissolve the dark blue crystals of formazan. Proliferation was determined using a Bio-Rad EIA reader (Bio-Rad, Hercules, CA) at a 570-nm wavelength.

BrdU labeling

The 95D cells transiently transfected with 10 nM miR-7 mimics or scramble control were treated with CpG ODNs as described previously (Xu *et al.*, 2010a). After 48 h, BrdU (5-bromo-2-deoxyuridine; Sigma-Aldrich) was added to a final concentration of 5 mmol/ml. After 4 h, 95D cells were collected and the proliferation was analyzed by fluorescence-activated cell sorting (FACS). In brief, cells (1×10^6 cells) were first incubated with fixation/permeabilization buffers for 45 min. After being washed twice, cells were incubated at 24°C for 30 min in 0.15 M NaCl, 4.2 mM $MgCl_2$, 10 mM HCl (pH 5) in the presence of 2 U DNase I (Invitrogen); this was followed by staining with α-BrdU for 30 min before cells were finally analyzed by FACS.

Flow cytometric analysis of cell cycle

The 95D cells were transiently transfected with 10 nM miR-7 mimics or scramble control using Lipofectamine 2000 (Invitrogen). Cells were then seeded at a density of 10^6 cells/100-mm dish in RPMI-1640 medium with 10% FBS for 48 h in the presence of CpG ODNs (10 µg/ml) or control. Then cells were washed with ice-cold PBS and harvested and fixed in 70% ethanol for 30 min. Cells were treated with RNase A and stained with 25 µg/ml propidium iodide (PI). Samples were analyzed using a FACScan flow cytometer (Becton Dickinson, San Jose, CA), according to the manufacturer's protocol.

Assessment of apoptosis by annexin V–fluorescein isothiocyanate

Apoptotic cell death was measured using a fluorescein isothiocyanate (FITC)-conjugated annexin V/PI assay kit by flow cytometry. Briefly, 5×10^5 cells were washed with ice-cold PBS, resuspended in 100 µl binding buffer, and stained with 5 µl of FITC-conjugated annexin V (10 mg/ml) and 10 µl of PI (50 mg/ml). The cells were incubated for 15 min at room temperature in the dark, 400 µl of binding buffer was added, and the cells were analyzed (FACScan; Becton Dickinson). The cells were gated separately according to their granularity and size on forward scatter versus side scatter plots. Early and late apoptosis was evaluated on fluorescence 2 (FL2 for PI) versus fluorescence 1 (FL1 for annexin) plots. Cells stained with only annexin V were evaluated as being in early apoptosis.

Wound-healing assays

The 95D cells were transiently transfected with 10 nm miR-7 mimics or scramble control as described above. Cells were then seeded in six-well plates at 1×10^5 per well in growth medium. Confluent monolayers were starved overnight in assay medium, and a single scratch wound was created using a micropipette tip. The cells were washed with PBS to remove cell debris, supplemented with assay medium containing 10 µg/ml CpG ODN, and monitored. Images were captured with a microscope at 0 and 24 h postwounding. For a quantitative measure, we counted the cells migrating to the wound area based on the image at 0 h postwounding.

data set for three independent experiments is shown. (B) The cell number of each group was also calculated. (C) The migration of 95D cells in each group was performed by Transwell assay, as described in *Materials and Methods*. (D) The invasion ability of 95D cells in each group also was determined by invasion assay. (E) The secretion of IL-8 from 95D cells in each group was determined by ELISA. (F) Groups of eight nude mice were challenged with 2×10^6 CpG ODN–pretreated 95D cells transfected with 100 µg miR-7 expression vector (pMir-7) or control vector (pCtrl) through the tail vein. After 30 d, the metastatic index was obtained. (G) Groups of eight nude mice were challenged with 2×10^6 95D cells transiently transfected with 100 µg miR-7 expression vector (pmir-7) or control vector (pCtrl). After 5 d, the tumor-bearing mice were injected in situ with 100 µg of CpG ODN at 7-d intervals. The control group received an equal dose of the control CpG ODN. After 30 d, the metastatic index was obtained. Each bar represented the means (± SD) from eight nude mice in each group. *, $p < 0.05$.

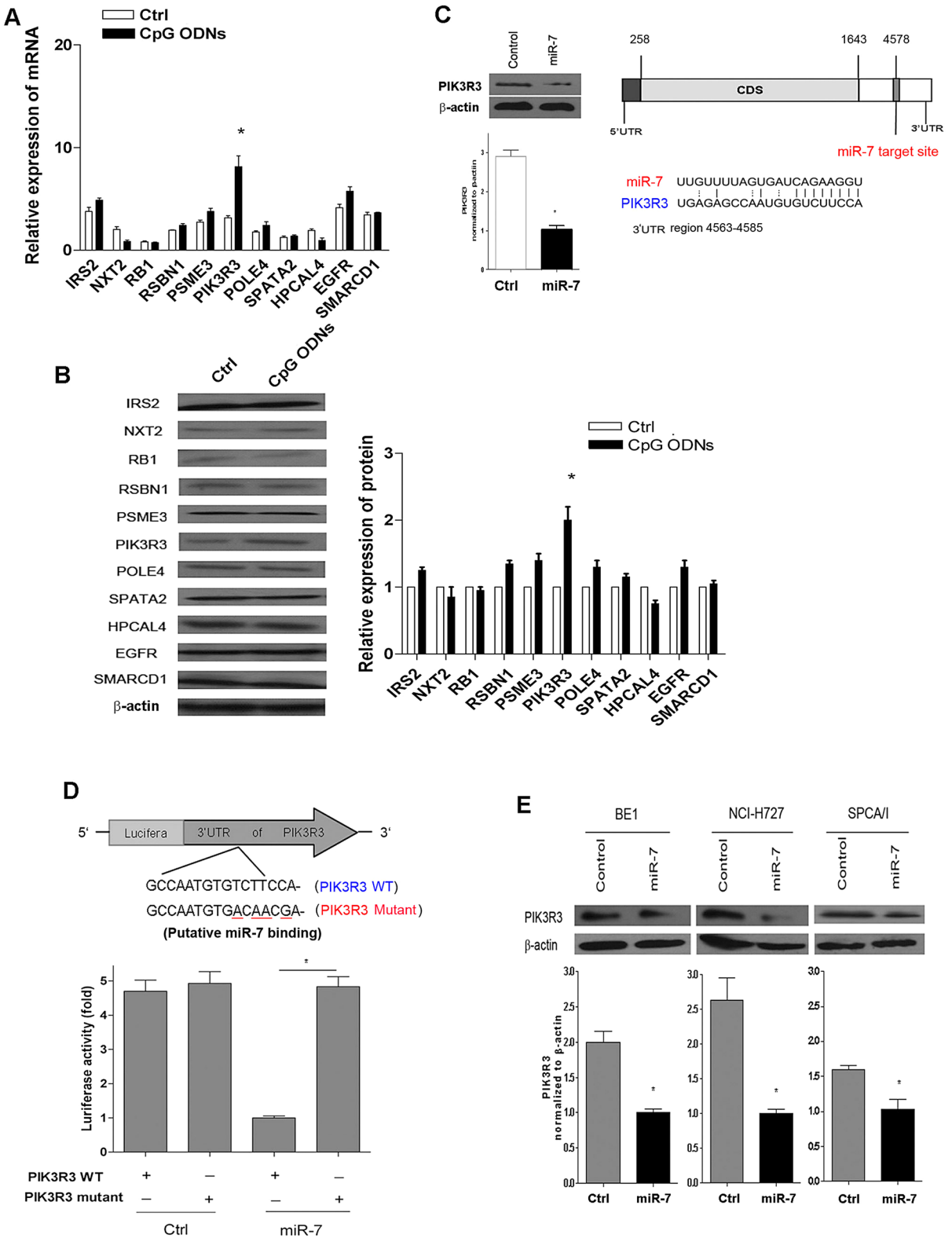

FIGURE 5: miR-7 repressed the expression of PIK3R3 in human lung cancer cells. The 95D cells were cultured in the presence of CpG ODN (10 μg/ml). After 48 h, the expression of 11 indicated genes was determined by RT-PCR (A) and Western blotting (B). (C) Sites of miR-7 seed matches in the PIK3R3 3′ UTR. The 95D cells (5×10^4 cells/well) were transiently transfected with 10 nM miR-7 mimics or scramble control for 48 h. The cells were then collected, and the expression of PIK3R3 was determined by Western blotting. (D) Luciferase assay of 95D cells was performed. Cells were transiently transfected with miR-7 mimics with or without plasmid pGL-PIK3R3 (PIK3R3 WT) or pGL-PIK3R3 mutation (PIK3R3 mutant). Cells were then cultured in a 96-well plate at 5×10^4 cells/well. After 24 h, the luciferase activity of each group was obtained. (E) The expression of PIK3R3 protein in human lung cancer cell line BE1, NCI-H727, and SPCA/I cells transiently transfected with miR-7 mimics were determined by Western blotting. *, $p < 0.05$.

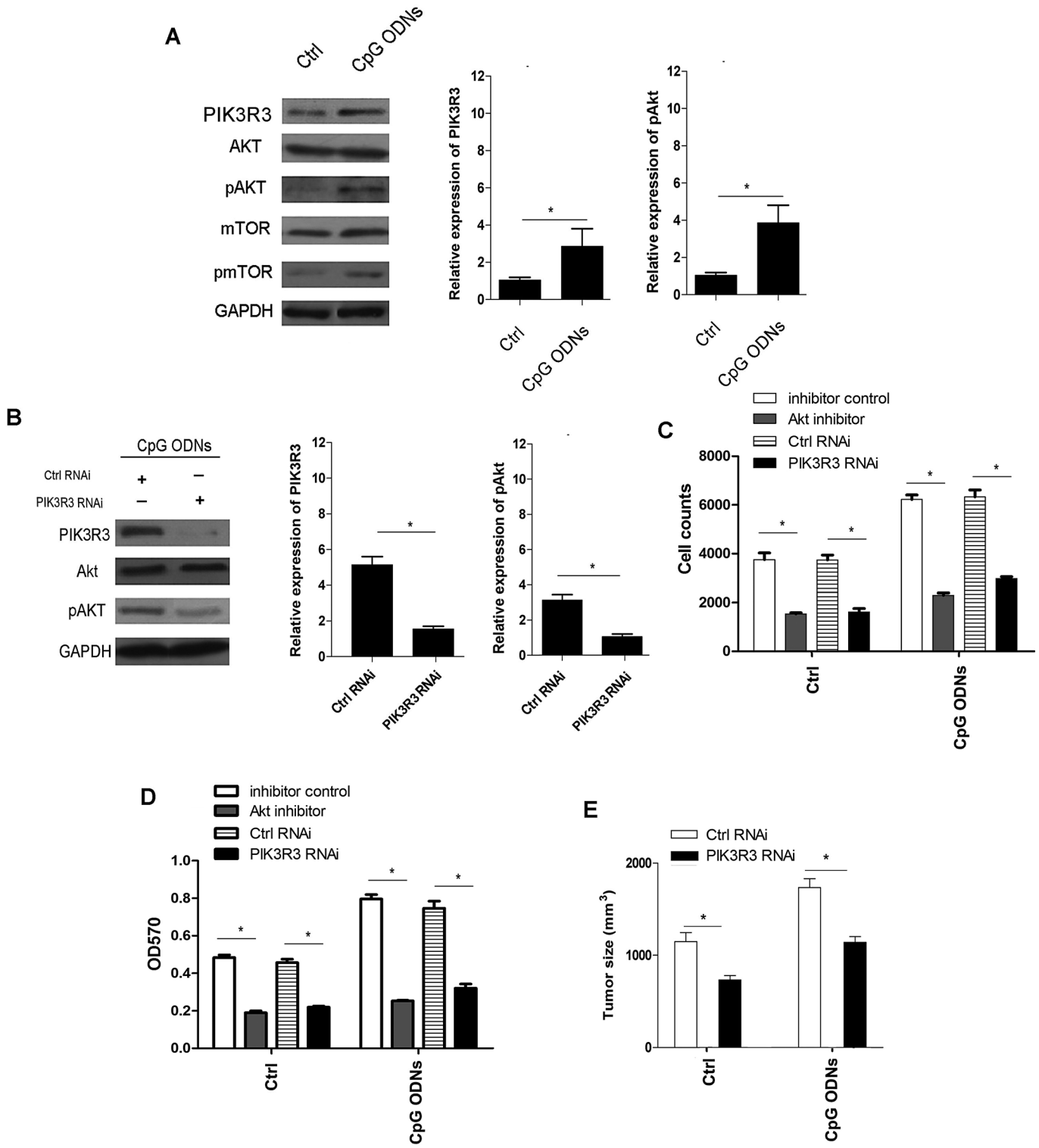

FIGURE 6: Down-regulation of PIK3R3 reduced the effect of TLR9 signaling on the growth of human lung cancer cells. (A) The 95D cells were treated with 10 μg/ml CpG ODN. After 24 h, the expression of PIK3R3 and Akt or pAkt were determined by Western blotting. (B) The 95D cells were transiently transfected with PIK3R3 RNAi (100 nmol) or control RNAi (100 nmol) and then treated with 10 μg/ml CpG ODN. After 24 h, the expression level of PIK3R3 and pAkt were detected by Western blotting. (C and D) The 95D cells were incubated in the presence of 1 μM Akt inhibitor IV or transiently transfected with PIK3R3 RNAi or control RNAi and then treated with 10 μg/ml CpG ODN for 72 h. Their growth was then analyzed as described in Figure 2. (E) Groups of eight nude mice were challenged with 2×10^6 95D cells transiently transfected with PIK3R3 RNAi. After 5 d, tumor-bearing mice were injected in situ with 100 μg CpG ODN or control CpG ODN at 7-d intervals. After 28 d, the tumor size was observed. *, $p < 0.05$.

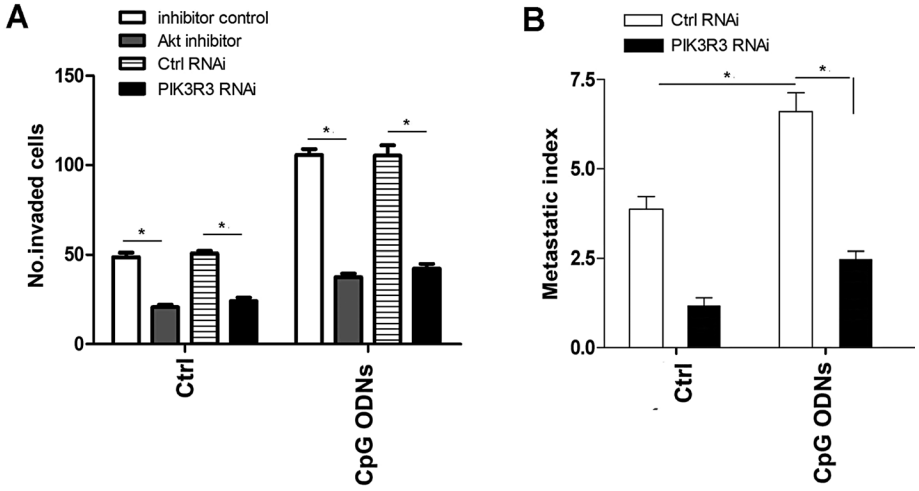

FIGURE 7: Down-regulation of PIK3R3 reduced the effect of TLR9 signaling on the metastatic potential of human lung cancer cells. (A) The 95D cells were incubated in the presence of (1 μM) Akt inhibitor IV or transiently transfected with PIK3R3 RNAi (100 nM) or control RNAi (100 nM) and then treated with 10 μg/ml CpG ODN. The cells' invasion capacity was then analyzed. (B) Groups of eight nude mice were challenged with 2×10^6 of 95D cells transiently transfected with PIK3R3 RNAi (100 nM) or control RNAi (100 nM). After 30 d, the metastatic index was obtained. Each bar represents the means (± SD) from eight nude mice in each group. *, $p < 0.05$.

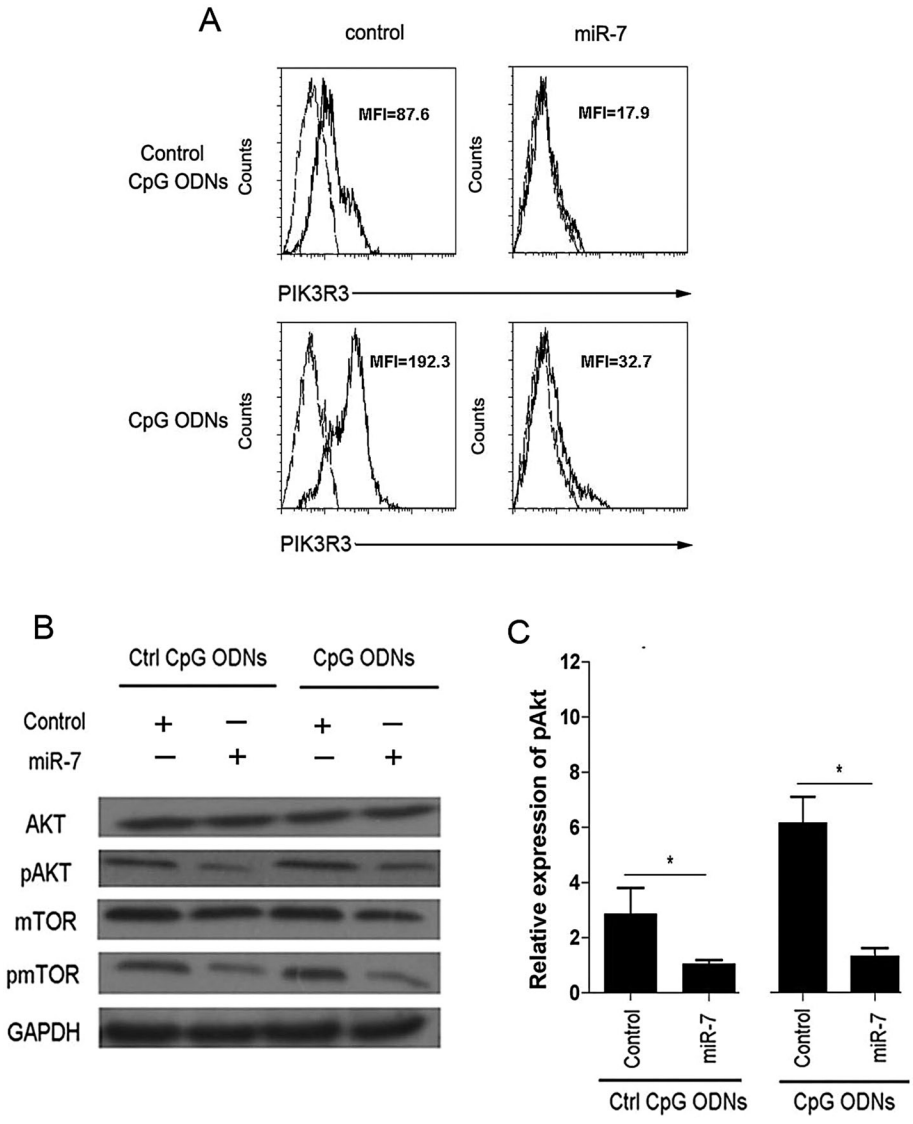

FIGURE 8: miR-7 regulated the transduction of the PIK3R3/Akt pathway in human lung cancer cells treated with CpG ODNs. (A) The 95D cells transiently transfected with miR-7 mimics (10 nM) were stimulated by CpG ODNs for 48 h. The expression level of PIK3R3 in 95D cells was analyzed by FACS. (B) The 95D cells transiently transfected with miR-7 mimics (10 nM) were stimulated by CpG ODNs for 48 h, then the expression level of pAkt and phosphor-mTOR on 95D cells were detected by Western blotting and calculated (C). *, $p < 0.05$.

Transwell migration assay

Cell migration assays were performed using a serum gradient in a modified Boyden chamber consisting of a cell culture insert (Lecomte *et al.*, 2011). Briefly, 95D cells were grown in starvation medium overnight prior to detachment, washed with PBS, and resuspended in the same medium. After being transiently transfected with miR-7 mimics or scramble control, single-cell suspensions of cells were prepared by filtration through a 35-μm mesh cell strainer (Becton Dickinson). Cells were counted, and a total of 1×10^6 cells suspended in serum-free medium were seeded onto the upper chamber of an insert and then positioned in a 24-well plate containing medium with or without 10% serum. When used, 10 μg/ml CpG ODN or control ODN was added to the medium in both chambers. Migration assays were carried out for 12 h at 37°C with 5% CO_2. Cells were then fixed with 3.7% formaldehyde, permeabilized with ice-cold methanol, and stained with a 0.2% crystal violet solution. Nonmigratory cells on the upper side of the insert were removed with a cotton swab. For quantification, five randomly selected fields on the lower side of the insert were counted through a 200× objective using computer-assisted microscopy and analyzed with CellProfiler 2.0 cell image-analysis software.

Invasion assay

The invasive assay was done in 24-well cell culture chambers using inserts with 8-μm pore membranes precoated with Matrigel (28Ag/insert; Sigma-Aldrich), as described previously (Xu *et al.*, 2009). The 95D cells transiently transfected with 10 nm miR-7 mimics or scramble control were placed in the upper wells in the presence of 10 μg/ml CpG ODN or control ODN, and the lower wells were filled with fibroblast-conditioned medium. After a 24-h incubation, cells on the lower surface of the membrane were stained by the hematoxylin and eosin (H&E) method and counted under a light microscope (400× objective).

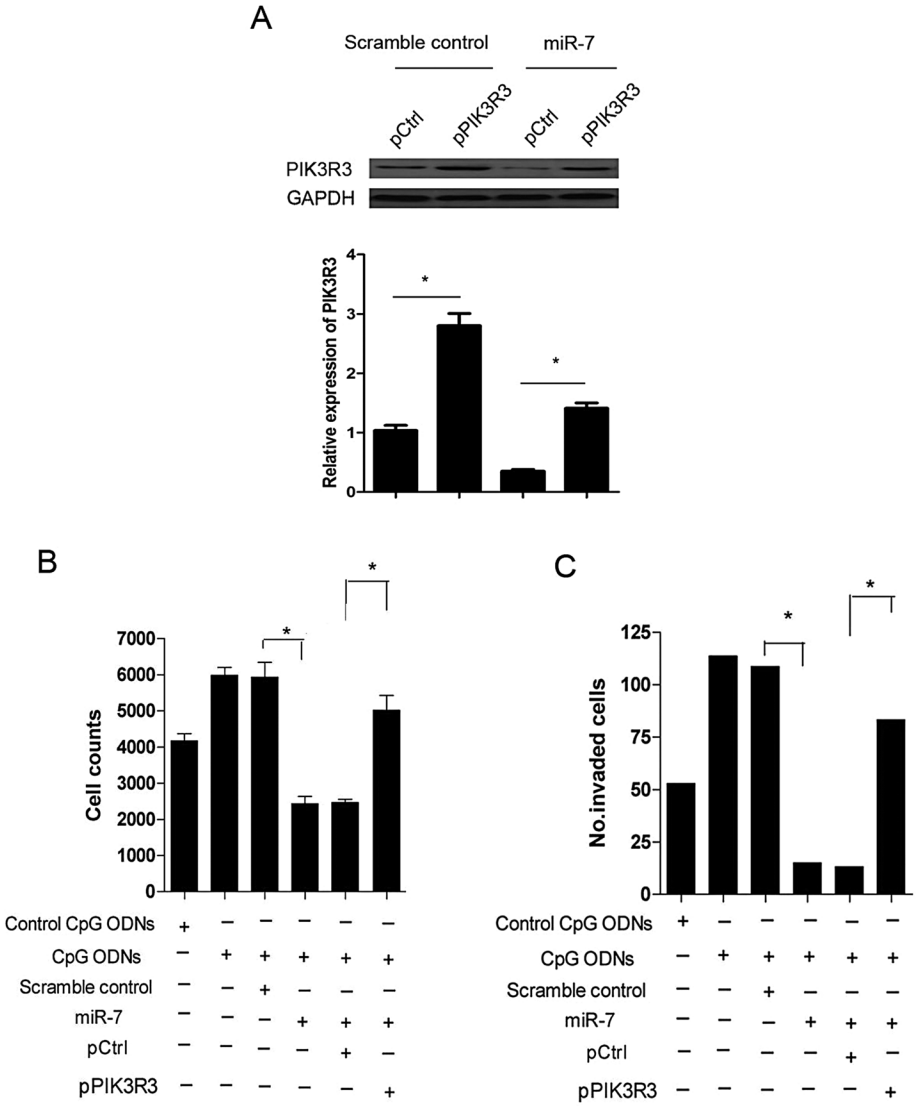

FIGURE 9: miR-7 regulated TLR9 signaling–enhanced growth and metastatic potential of 95D cells through PIK3R3/Akt pathway. (A) The 95D cells were transiently cotransfected with pPIK3R3 (100 μg) or control vectors (100 μg) with or without miR-7 mimics (10 nM). After 48 h, the expression of PIK3R3 in 95D cells was determined by Western blotting. (B) The 95D cells were transiently cotransfected with pPIK3R3 (100 μg) or control vectors (100 μg) with or without miR-7 mimics (10 nM). Cells were then stimulated with 10 μg/ml CpG ODN in vitro. The growth of cells was detected by MTT assay. (C) The invasive capacity of cells also was detected by invasion assay. *, $p < 0.05$.

ELISA

The 95D cells transiently transfected with 10 nm miR-7 mimics or scramble control were seeded at 3×10^3 cells per well and incubated in the presence or absence of CpG ODN at a dose of 10 μg/ml at 37°C in 5% CO_2 in a 96-well plate for 72 h. The supernatant concentration of IL-8 was determined using commercial enzyme-linked immunosorbent assay (ELISA) kits for human IL-8 (BD Biosciences, Franklin Lakes, NJ). Samples (culture supernatants) were collected from replicated cultures and measured without dilution.

Luciferase plasmid construction

Plasmid pGL3-PIK3R3-luc (pPIK3R3 WT) was generated by cloning annealed ODNs corresponding to nucleotides 4563–4585 of *PIK3R3* (GenBankTM accession number: BC021622.1) mRNA 3′ UTR into *Xba*I and *Hpa*I sites in pGL3 control vector. Plasmid pGL3-PIK3R3-mutation (pPIK3R3-Mutant) contained a PCR-generated *PIK3R3* 3′-UTR sequence that included four nucleotide substitutions to impair binding of the miR-7 seed sequence to its target. The sequence of all plasmids was confirmed by sequencing.

Luciferase reporter assay

The 95D cells were transiently cotransfected with plasmids pPIK3R3 Luc and pCMV-lacZ plasmids using Lipofectamine 2000 (Invitrogen) according to the manufacturer's instruction, and cultured in the presence of 10 μg/ml CpG ODNs. After 24 h, luciferase and β-gal activity in 100 μl of cell lysates were measured by the Luciferase Assay System and the Galactosidase Enzyme Assay System (Promega, Madison, WI), respectively. Transfection efficiency was normalized using β-gal activity.

In vivo metastasis assay

The effects of miR-7 on TLR9 signaling–enhanced metastasis of 95D cells in vivo was performed as described previously with some modification (Xu *et al.*, 2009). The 95D cells (5×10^6) transiently transfected with 100 μg pMir-7 or control vector were pretreated with 10 μg/ml CpG ODNs. After 3 d, the cells were collected and then injected into the tail veins of nude mice. Each treatment was administered to a group of eight mice. At 30-d postinjection, the mice were killed and the lungs were harvested in optimum cutting-temperature compound and frozen in liquid nitrogen. The collected lung tissue sections were subjected to H&E histostaining. The metastatic index was calculated based on the number and diameter of metastatic foci of lung.

Western blotting

Western blotting was performed on cytosolic cellular extracts. Equal amounts of protein were resolved under reducing conditions on a 10% SDS–PAGE. Protein migration was assessed using protein standards (Bio-Rad). Transfer to a nitrocellulose membrane was performed overnight at 30 V using a wet transfer system. Equal protein loading was confirmed with Ponceau staining. The membrane was washed in 5% skim milk in phosphate-buffered saline (PBS) plus 0.03% Tween 20 (PBS-T) for 1 h in order to block nonspecific protein-binding sites on the membrane. Immunoblotting was performed using a monoclonal antibody to PIK3R3 (55036-1-AP; Proteintech, Chicago, IL), Akt (ab28422; Abcam, Cambridge, MA), mTOR (ab2833; Abcam), pAkt (ab8932; Abcam), phosphor-mTOR (ab1093; Abcam), IRS-2 (sc-1555; Santa Cruz Biotechnology, Santa Cruz, CA), NXT2 (ab121797; Abcam), Rb1 (Santa Cruz, sc-73598; Santa Cruz Biotechnology), RSBN1 (ab102071; Abcam), PSME3 (ab97576; Abcam), POLE4 (ARP39392_P050; Aviva Systems Biology, San Diego, CA), SPATA2 (ab56565; Abcam), EGFR (ab2430; Abcam), HPCAL4 (ab106767; Abcam), and SMARCD1 (ab83208;

Gene	Primers
IRS2	Up: 5′-TACCGTCTGTGCCTGTCTGC-3′
	Down: 5′-CGACGATTGGCTCTTACTGC-3′
NXT2	Up: 5′ AAAGAAGACGGGCACT-3′
	Down: 5′ AAACGGAAGCAATCAC-3′
Rb1	Up: 5′-AGGACCCAGAGCAGGAC-3′
	Down: 5′-CTCCCAATACTCCATCCAC-3′
RSBN1	Up: 5′-TCTCGTTGGAGCAGTAG-3′
	Down: 5′-TTCATTGATCGTCGTCT-3′
PSME3	Up: 5′-CAGAAGACTTGGTGGCA-3′
	Down: 5′-GTCAGGGACTGGGAGA-3′
PIK3R3	Up: 5′-GGTGATGATGCCCTAT-3′
	Down: 5′-TCCGCAAAGTCAAAGTA-3′
POLE4	Up: 5′-AGGCCCCAACGAGTGT-3′
	Down: 5′-GATGGCTTCCTGTCCC-3′
SPATA2	Up: 5′-GTGGCAGCCTCAACCCT-3′
	Down: 5′-GCTCGGAGTAGCCCTTG-3′
HPCAL4	Up: 5′-ACGCTTTCCGCACCTT-3′
	Down: 5′-CTCTTGGCTGCCTCCT-3′
EGFR	Up: 5′-TCTCCGAAAGCCAACA-3′
	Down: 5′-GACGGTCCTCCAAGTAG-3′
SMARCD1	Up: 5′-TTCGGGTAGAAGGACG-3′
	Down: 5′-TGGACGAGTCTGGGTAT-3′
miR-7	Up: 5′-GACTAGTGATTTTGTT-3′
	Down: 5′-ACCTTCTGATCACTAA-3′

TABLE 1: The primers used for target genes.

Abcam) at a dilution of 1:1000 in a nonfat milk–Tris buffer. The membrane was then washed in PBS-T and subsequently probed with a corresponding secondary anti–rabbit antibody or anti–mouse antibody conjugated to horseradish peroxidase (Amersham Life Sciences, Piscataway, NJ) at a dilution of 1:5000 and developed with chemiluminescence (Pierce, Rockford, IL). The membrane was then exposed to x-ray film (Kodak, Rochester, NY), which was subsequently developed.

Evaluation of tumor growth in vivo

Evaluation of tumor growth was performed as described previously (Ren *et al.*, 2009). Briefly, BALB/c nu/nu mice (6–8 wk old) were injected subcutaneously with 0.2 ml of a single-cell suspension containing 2×10^6 tumor cells and kept in laminar flow cabinets under specific pathogen-free conditions. Tumors were measured every 3 or 4 d following tumor challenge using vernier calipers. Tumor volumes were obtained by multiplying the measured length by the measured width by the calculated mean of these measured values and are presented as the mean ± SEM.

Histopathology

Lung tissues were fixed in 4% paraformaldehyde, embedded in paraffin, and cut into 5-μm-thick sections. Sections were stained with hematoxylin and eosin, and images were taken with a Nikon Eclipse E800 microscope.

Statistical analyses

Statistical analyses of the data were performed with the aid of analysis programs in SPSS 12.0 software. Statistical evaluation was performed with one-way analysis of variance ($p < 0.05$) using Prism 5.0 (GraphPad, San Diego, CA).

ACKNOWLEDGMENTS

This work was supported by the National Natural Science Foundation of China (81071744, 81260398), the International Cooperation Foundation of Guizhou Province (2010-7031), the Shanghai Rising-Star Follow-Up Program (10QH1402000), the Specific Foundation for the Scientific Educational Talent of President of Guizhou Province (09C457, 10-49), the Fund of Science and Technology Commission of Shanghai Municipality (09411966400), the Shanghai Pudong New Area Academic Leader in Health System (PWRd2010-01), the Project of Guizhou provincial Department of Science and Technology (2009C491), and the Zunyi Medical College Start-up Fund (2008F-329).

REFERENCES

Ahmad R, Sylvester J, Zafarullah M (2007). MyD88, IRAK1 and TRAF6 knockdown in human chondrocytes inhibits interleukin-1-induced matrix metalloproteinase-13 gene expression and promoter activity by impairing MAP kinase activation. Cell Signal 19, 2549–2557.

Bhattacharya D, Yusuf N (2012). Expression of toll-like receptors on breast tumors: taking a toll on tumor microenvironment. Int J Breast Cancer 2012, 716564.

Bomben R *et al.* (2012). The miR-17-92 family regulates the response to Toll-like receptor 9 triggering of CLL cells with unmutated IGHV genes. Leukemia 26, 1584–1593.

Cammarota R *et al.* (2010). The tumor microenvironment of colorectal cancer: stromal TLR-4 expression as a potential prognostic marker. J Transl Med 8, 112.

Ceppi M, Pereira PM, Dunand-Sauthier I, Barras E, Reith W, Santos MA, Pierre P (2009). MicroRNA-155 modulates the interleukin-1 signaling pathway in activated human monocyte-derived dendritic cells. Proc Natl Acad Sci USA 106, 2735–2740.

Chen R, Alvero AB, Silasi DA, Kelly MG, Fest S, Visintin I, Leiser A, Schwartz PE, Rutherford T, Mor G (2008a). Regulation of IKKβ by miR-199a affects NF-κB activity in ovarian cancer cells. Oncogene 27, 4712–4723.

Chen R, Alvero AB, Silasi DA, Steffensen KD, Mor G (2008b). Cancers take their Toll—the function and regulation of Toll-like receptors in cancer cells. Oncogene 27, 225–233.

Creagh EM, O'Neill LA (2006). TLRs, NLRs and RLRs: a trinity of pathogen sensors that co-operate in innate immunity. Trends Immunol 27, 352–357.

Droemann D, Albrecht D, Gerdes J, Ulmer AJ, Branscheid D, Vollmer E, Dalhoff K, Zabel P, Goldmann T (2005). Human lung cancer cells express functionally active Toll-like receptor 9. Respir Res 6, 1.

Esquela-Kerscher A, Slack FJ (2006). Oncomirs—microRNAs with a role in cancer. Nat Rev Cancer 6, 259–269.

Fang Y, Xue JL, Shen Q, Chen J, Tian L (2012). miR-7 inhibits tumor growth and metastasis by targeting the PI3K/AKT pathway in hepatocellular carcinoma. Hepatology 55, 1852–1862.

González-Reyes S, Fernández JM, González LO, Aguirre A, Suárez A, González JM, Escaff S, Vizoso FJ (2011). Study of TLR3, TLR4, and TLR9 in prostate carcinomas and their association with biochemical recurrence. Cancer Immunol Immunother 60, 217–226.

Guo D, Ye J, Dai J, Li L, Chen F, Ma D, Ji C (2009). Notch-1 regulates Akt signaling pathway and the expression of cell cycle regulatory proteins cyclin D1, CDK2 and p21 in T-ALL cell lines. Leuk Res 33, 678–685.

He W, Liu Q, Wang L, Chen W, Li N, Cao X (2007). TLR4 signaling promotes immune escape of human lung cancer cells by inducing immunosuppressive cytokines and apoptosis resistance. Mol Immunol 44, 2850–2859.

Hu J, Xia X, Cheng A, Wang G, Luo X, Reed MF, Fojo T, Oetting A, Gong J, Yen PM (2008). A peptide inhibitor derived from p55PIK phosphatidylinositol 3-kinase regulatory subunit: a novel cancer therapy. Mol Cancer Ther 7, 3719–3728.

Huang B, Zhao J, Li H, He KL, Chen Y, Chen SH, Mayer L, Unkeless JC, Xiong H (2005). Toll-like receptors on tumor cells facilitate evasion of immune surveillance. Cancer Res 65, 5009–5014.

Ioannou S, Voulgarelis M (2011). Toll-like receptors, tissue injury, and tumourigenesis. Mediators Inflamm. doi:10.1155/2010/581837.
Kirigin FF *et al.* (2012). Dynamic microRNA gene transcription and processing during T cell development. J Immunol 188, 3257–3267.
Kong D *et al.* (2011a). Liposomal delivery of MicroRNA-7-expressing plasmid overcomes epidermal growth factor receptor tyrosine kinase inhibitor-resistance in lung cancer cells. Mol Cancer Ther 10, 1720–1727.
Kong D *et al.* (2011b). Inflammation-induced repression of tumor suppressor miR-7 in gastric tumor cells. Oncogene 31, 3949–3960.
Lecomte N, Njardarson JT, Nagorny P, Yang G, Downey R, Ouerfelli O, Moore MA, Danishefsky SJ (2011). Emergence of potent inhibitors of metastasis in lung cancer via syntheses based on migrastatin. Proc Natl Acad Sci USA 108, 15074–15078.
Lim EJ, Park DW, Jeong TW, Chin BR, Bae YS, Baek SH (2012). TRAIL is involved in CpG ODN-mediated anti-apoptotic signals. Oncol Rep 27, 1213–1218.
Lin P, Sun X, Feng T, Zou H, Jiang Y, Liu Z, Zhao D, Yu X (2012). ADAM17 regulates prostate cancer cell proliferation through mediating cell cycle progression by EGFR/PI3K/AKT pathway. Mol Cell Biochem 359, 235–243.
Liu G, Friggeri A, Yang Y, Park YJ, Tsuruta Y, Abraham E (2009). miR-147, a microRNA that is induced upon Toll-like receptor stimulation, regulates murine macrophage inflammatory responses. Proc Natl Acad Sci USA 106, 15819–15824.
Majumder S, Jacob ST (2011). Emerging role of microRNAs in drug-resistant breast cancer. Gene Expr 15, 141–151.
Min R, Zun Z, Siyi L, Wenjun Y, Lizheng W, Chenping Z (2011). Increased expression of Toll-like receptor-9 has close relation with tumour cell proliferation in oral squamous cell carcinoma. Arch Oral Biol 56, 877–884.
Mínguez B, Lachenmayer A (2011). Diagnostic and prognostic molecular markers in hepatocellular carcinoma. Dis Markers 31, 181–190.
Nahid MA, Satoh M, Chan EK (2011). Mechanistic role of microRNA-146a in endotoxin-induced differential cross-regulation of TLR signaling. J Immunol 186, 1723–1734.
Patron JP *et al.* (2012). MiR-133b targets antiapoptotic genes and enhances death receptor-induced apoptosis. PloS One 7, e35345.
Pinto A, Morello S, Sorrentino R (2011). Lung cancer and Toll-like receptors. Cancer Immunol Immunother 60, 1211–1220.
Ravindran C, Cheng YC, Liang SM (2010). CpG-ODNs induces up-regulated expression of chemokine CCL9 in mouse macrophages and microglia. Cell Immunol 260, 113–118.
Rebane A (2011). microRNA expression profiles of human blood monocyte derived dendritic cells and macrophages reveal miR-511 as putative positive regulator of TLR4. J Biol Chem 286, 26487–26495.
Reddy SD, Ohshiro K, Rayala SK, Kumar R (2008). MicroRNA-7, a homeobox D10 target, inhibits p21-activated kinase 1 and regulates its functions. Cancer Res 68, 8195–8200.
Ren T, Wen ZK, Liu ZM, Liang YJ, Guo ZL, Xu L (2007). Functional expression of TLR9 is associated to the metastatic potential of human lung cancer cell. Cancer Biol Ther 6, 1704–1709.
Ren T, Xu L, Jiao S, Wang Y, Cai Y, Liang Y, Zhou Y, Zhou H, Wen Z (2009). TLR9 signaling promotes tumor progression of human lung cancer cell in vivo. Pathol Oncol Res 15, 623–630.
Samara KD, Antoniou KM, Karagiannis K, Margaritopoulos G, Lasithiotaki I, Koutala E, Siafakas NM (2012). Expression profiles of Toll-like receptors in non-small cell lung cancer and idiopathic pulmonary fibrosis. Int J Oncol 40, 1397–1404.
Saydam O *et al.* (2011). miRNA-7 attenuation in Schwannoma tumors stimulates growth by upregulating three oncogenic signaling pathways. Cancer Res 71, 852–861.
Sheedy FJ, Palsson-McDermott E, Hennessy EJ, Martin C, O'Leary JJ, Ruan Q, Johnson DS, Chen Y, O'Neill LA (2010). Negative regulation of TLR4 via targeting of the proinflammatory tumor suppressor PDCD4 by the microRNA miR-21. Nat Immunol 11, 141–147.
Song C, Chen LZ, Zhang RH, Yu XJ, Zeng YX (2006). Functional variant in the 3'-untranslated region of Toll-like receptor 4 is associated with nasopharyngeal carcinoma risk. Cancer Biol Ther 5, 1285–1291.
Soroceanu L *et al.* (2007). Identification of IGF2 signaling through phosphoinositide- 3-kinase regulatory subunit 3 as a growth-promoting axis in glioblastoma. Proc Natl Acad Sci USA 104, 3466–3471.
Sorrentino R, Morello S, Giordano MG, Arra C, Maiolino P, Adcock IM, Pinto A (2011). CpG-ODN increases the release of VEGF in a mouse model of lung carcinoma. Int J Cancer 128, 2815–2822.
Troutman TD, Hu W, Fulenchek S, Yamazaki T, Kurosaki T, Bazan JF, Pasare C (2012). Role for B-cell adapter for PI3K (BCAP) as a signaling adapter linking Toll-like receptors (TLRs) to serine/threonine kinases PI3K/Akt. Proc Natl Acad Sci USA 109, 273–278.
Tserel L, Runnel T, Kisand K, Pihlap M, Bakhoff L, Kolde R, Peterson H, Vilo J, Peterson P, Rebane A (2011). MicroRNA expression profiles of human blood monocyte-derived dendritic cells and macrophages reveal miR-511 as putative positive regulator of Toll-like receptor 4. J Biol Chem 286, 26487–26495.
Tsushima F, Tanaka K, Otsuki N, Youngnak P, Iwai H, Omura K, Azuma M (2006). Predominant expression of B7-H1 and its immunoregulatory roles in oral squamous cell carcinoma. Oral Oncol 42, 268–274.
Wang CC, Zeng Q, Hwang LA, Guo K, Li J, Liew HC, Hong W (2006). Mouse lymphomas caused by an intron-splicing donor site deletion of the FasL gene. Biochem Biophys Res Commun 349, 50–58.
Webster RJ, Giles KM, Price KJ, Zhang PM, Mattick JS, Leedman PJ (2009). Regulation of epidermal growth factor receptor signaling in human cancer cells by microRNA-7. J Biol Chem 284, 5731–5741.
Wendlandt EB, Graff JW, Gioannini TL, McCaffrey AP, Wilson ME (2012). The role of microRNAs miR-200b and miR-200c in TLR4 signaling and NF-κB activation. Innate Immun, doi: 10.1177/1753425912443903.
Xiong S, Zheng Y, Jiang P, Liu R, Liu X, Chu Y (2011). MicroRNA-7 inhibits the growth of human non-small cell lung cancer A549 cells through targeting BCL-2. Int J Biol Sci 7, 805–814.
Xu L, Wang C, Wen Z, Yao X, Liu Z, Li Q, Wu Z, Xu Z, Liang Y, Ren T (2010a). Selective upregulation of CDK2 is critical for TLR9 signaling stimulated proliferation of human lung cancer cell. Immunol Lett 127, 93–99.
Xu L, Wang C, Wen Z, Zhou Y, Liu Z, Liang Y, Xu Z, Ren T (2010b). CpG oligodeoxynucleotides enhance the efficacy of adoptive cell transfer using tumor infiltrating lymphocytes by modifying the Th1 polarization and local infiltration of Th17 cells. Clin Dev Immunol 2010, 410893.
Xu L, Zhou Y, Liu Q, Luo JM, Qing M, Tang XY, Yao XS, Wang CH, Wen ZK (2009). CXCR4/SDF-1 pathway is crucial for TLR9 agonist enhanced metastasis of human lung cancer cell. Biochem Biophys Res Commun 382, 571–576.
Zhang L *et al.* (2007). Integrative genomic analysis of phosphatidylinositol 3'-kinase family identifies PIK3R3 as a potential therapeutic target in epithelial ovarian cancer. Clin Cancer Res 13, 5314–5321.